UAV imagery based tree species classification in the Marburg OpenForest

Darius A. Görgen Tobias Koch Marvin Müsgen Eike Schott

April 05, 2020

Abstract

The monitoring of forests environments is of crucial importance since they serve as natural habitats and constitute a main source of biological diversity on the planet. Yet, it is very costly and labor intensive to monitor forests by traditional means and classical remote sensing technologies restrict the analysis to the regional level. To overcome these challenges there have been several attempts to use UAV-borne imagery in forest monitoring. By the use of drones images can be obtained at low cost and can be associated with both, high spatial and temporal resolution. This enables scientists and practitioners to comprehensively monitor forest environments. In this paper we present our results of an experiment exploring the influence of spatial resolution of RGB imagery, artificially derived vegetation indices as well as seasonal parameters on the accuracy of tree species classification within the Marburg OpenForest. We used a resolution of 10, 15, and 25 cm in a forward-feature-selection based on the Random Forest classification algorithm. Additionally we tested the obtained accuracy when only mono-temporal or multi-temporal variables are included as well as both types of variables. Our results show that accuracy is prone to errors in pixel georeferencing and tree location. Object-based classification methods might lead to higher classification accuracies, but the construction of balanced traning dataset is of preelminary importance and needs further improvment for our study area.

Contents

1 Introduction

Forests environments provide valuable services to the human well being as well as supporting services to the function of ecosystems. Additionally, they count to the main biodiversity hotspots on earth (Brockerhoff et al., 2017). However, the most recent Global Forest Resource Assessment of the FAO states, that the global forest area shrinked between 1990 and 2015 from 31.6% of the global land cover to 30.6%, or in other numbers from 4,128 Mio. ha to 3,999 Mio. ha - a decrease of 3.1% (Food and Agriculture Organsiation of the United Nations, 2015). Simultaneously, the percentage of planted trees increased by over 105 Mio. ha, reducing the share of natural forest areas. Over the last decades, we can find growing scholar interests on ecosystem services and functions which are sustained by forests, mainly the habitat provision for endangered or native species, the provision of material goods such as wood biomass, soil formation and composition, as well as climatic regulation functions, such as carbon sequestration (Brockerhoff et al., 2017). One of the main critical variables in assessing the quality of forest environments, their biodiversity, and their structural attributes is the tree species, either on the individual tree level or the dominating species for coarser areas of interest.

Identifying tree species, however, on an operative scale for larger areas, remains a challenge. Recently, different remote sensing approaches proved that tree species identification from above the earth's surface is feasible, but there still remain significant trade-offs between the costs, computational demand and spatial-temporal resolution of remotely sensed imagery. Some studies have used satellite imagery which most frequently also include information in the infrared spectrum (Elatawneh et al., 2013; Grabska et al., 2019; Persson et al., 2018; Ulsig et al., 2017; Zhang et al., 2003) but generally shows a relatively low spatial resolution limiting the analysis to a level of stand rather than individuals. Additionally, depended on the platform's orbit and current weather conditions, the temporal resolution may vary significantly and is not completely planable.

One technology to partly overcome these restrictions is the use of Radio Detection And Ranging (RADAR) sensors which show a lower dependency of data quality to the presence of clouds and fog. Recently, multi-temporal data from Sentinel-1 has been used in conjunction with spectral data to not only improve the species classification accuracy but also to retrieve additional parameters important to forest monitoring such as forest type, stand density, annual phenology, and biomass production among others (Dostálová et al., 2018; Frison et al., 2018; Mngadi et al., 2019; Niculescu et al., 2018). However promising these advances, the analysis are most commonly restricted to regional analysis of forest structures. On a more localized level, high resolution satellite data is either not available or associated with very high costs. With the rapid development of unmanned aerial vehicles (UAV) during the last years and a significant decrease in price for this technology, new approaches to monitor forest structures on a very local level have recently emerged (Yao et al., 2019).

UAVs serve as an aerial platform of different kind of sensors which can range from LidAR (Fricker et al., 2019), hyper- and multi spectral sensors (Berra et al., 2019; Marques et al., 2019) as well as simple RGB cameras (Natesan et al., 2019). A broad methodology to obtain species information for single tree individuals has been developed integrating the calculation of various vegetation indices from mono- and multi-temporal imagery and the use of machine learning models to derive a relationship between the measured variables and the tree species. Berra et al. (2016) used the Green Chromatic Coordinate to monitor the Start-of-Season for four different tree species in deciduous woodland suggesting that UAV imagery can contribute to investigate the phenological status of individual trees. Klosterman and Richardson (2017) were able to estimate phenological status on the leaf-level based on the calculation of the green and red chromatic coordinate (GCC and RCC) during spring and autumn to bud burst and leaf expansion as well as leaf senescence. Natesan et al. (2019) used Residual Neural Networks to classify three different tree species based on RGB imagery obtained over the course of three years and achieved a classification accuracy of about 80%, and an accuracy of 51% when only the data of single years was used. Fricker et al. (2019) used hyperspectral images obtained by a UAV and a Convolutional Neural Network to classify tree species. They also underwent an experiment which only included RGB data. The hyperspectral data achieved an F-score of 0.87, while the RGB data achieved a score of 0.64 in a dominantly coniferous forest.

Additionally, the development of structure-from-motion algorithms to get 3D information from 2D RGB imagery taken from slightly different angles have enriched the analysis of forest structures from low-cost sensors. Nevalainen et al. (2017) used RGB images and an automated matching technique to obtain point clouds at a 5cm resolution. Coupled with hyperspectral imagery this allowed the tree species classification to an accuracy at 95%. Yan et al. (2018) compared their approach of retrieving tree crowns from RGB images with crowns delineated from LiDAR data and report an accuracy at about 90%. Krause et al. (2019) were able to retrieve individual tree height based on a photogrammetric point-cloud with an RMSE at about 2-3 %. Brieger et al. (2019) used RGB derived point clouds at different study sites in Siberia and achieved an accuracy of 67.1% in delineating individual tree crowns and an RMSE of 18.46% for tree height. Sothe et al. (2019) used hyperspectral images for tree delineation and classification in subtropical rain forests and achieved and Kappa score of 0.7 (overall accuracy of 72.4%) by combining spectral raw data, indices as well as structural parameters in the classification process using a support-vector machine.

However, little efforts have been done to structurally investigate the impact of decreasing spatial resolution on the classification accuracy as well as the impact of the integration of seasonal parameters derived from multiple mono-temporal observations. Here, we strictly limit our analysis to the investigation of these two thematic blocs and deliberately exclude other factors such as structural variables obtained from point clouds. We solely focus on the analysis of the dynamic in predictive potential of RGB derived mono- and multi-temporal variables to model tree species with changing spatial resolution.

To this end we use the RGB imagery obtained by multiple overflights during the year 2019 from a study side located within the Marburg University forest which is part of the research project Natur 4.0. This forest is used as a joint research area for a project between several German universities and research institutes and sets out to investigate the potential of sensor technology for biodiversity and natural resource management in natural environments forests. We artificially decreased the spatial resolution of aerial imagery obtained in this area resulting in three different target resolutions of 10, 15, and 25 cm. For every single overflight we calculated a series of RGB indices on a pixels basis. Additionally, we calculate descriptive statistics (mean, maximum, minimum, amplitude, etc.) for each index over the course of the year to include information about the seasonality of the phenological development.

The resulting input data is used to establish a total of nine distinct random forest models, one for each resolution including either only mono-temporal or seasonal predictor variables or both types of variables. On the basis of a forward-feature selection the variables which carry the most relevant information content for the tree species classification are then selected and used in the species prediction. The evaluation of the classification accuracies is compared on a pixel and object basis to draw conclusions on the importance of spatial resolution as well as the importance of mono- vs. multi-temporal input data.

2 Data and Methods

2.1 Study Area

The study area is located at 50.8°N 8.7°E in the German low mountain range in Hesse. It is part of the University Forest Caldern where the recently initiated joint research project Natur 4.0 aims at investigating the use of networked sensor technology for biodiversity and ecosystem management and protection. It is in this context, that the aerial images which we used here were obtained in an observation campaign during 2019 (see Tab. 1). The area is approximately 37,500 m^2 and continuously covered by trees. In this specific location, only two distinct species are present with stem diameters at breast height (DBH) greater than 40 cm, namely *fagus sylvatica* and *quercus robur*.

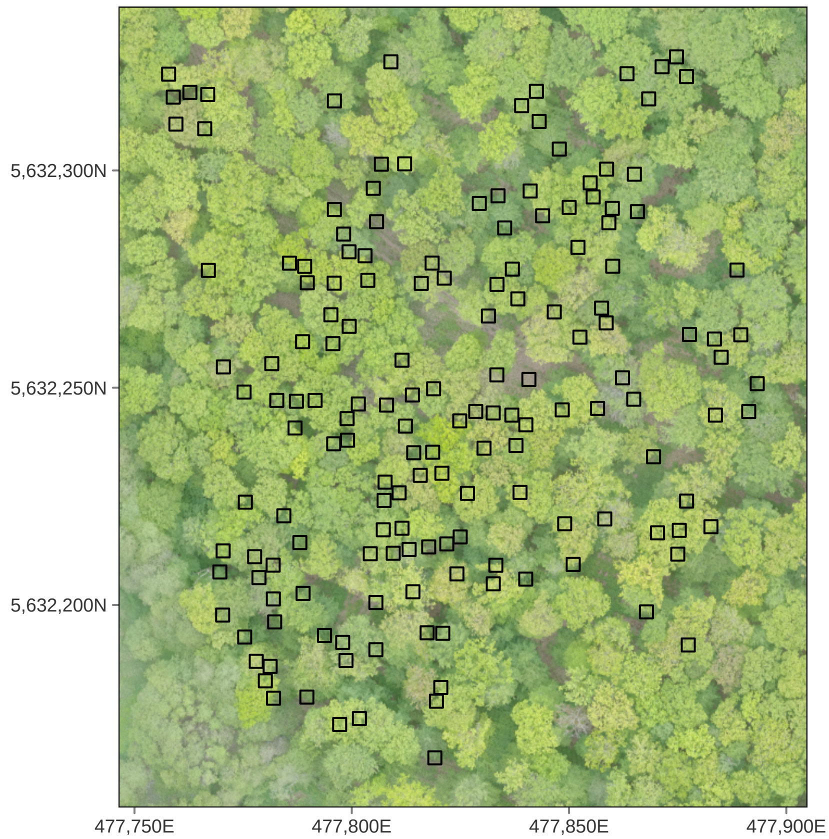

Figure 1: RGB image of the study area from May 16th 2019 with central positions of tree stems superimposed (Coordinates are presented in UTM32N).

2.2 Pre-Processing of the UAV orthoimages

In this project, AgisoftPhotoScan was used to process the UAV imagery. Agisoft Photoscan Professional is an affordable 3D reconstruction software from the Russian company Agisoft LLC Agisoft (2019) for the generation of dense point clouds and photogrammetric products such as orthorectified mosaics and DSM derived from images. Photoscan has the advantage to provide a simple workflow, from performing bundle block adjustment to calibrate the camera and orientate images after automatic tie point measurements, geo-referencing by measuring ground control points, concluding with the computation of a dense point cloud and requested final products (Mayer and Kersten, 2018). The Airborne system was used to acquire the UAV imagery using a commercial GoPro in several flight campaigns with a flight altitude of 40 meters The internal GPS of the GoPro was used for geotagging the images. A post referencing enabled a better processing of the images in SFM software and more accurate orthophotos without manual referencing in Photoscan. Photo Alignment is a process in PS for image matching and bundle block adjustment in an arbitrary system. It generates a sparse point cloud as well as the interior and exterior orientation parameters of all images in that system, including systematic error compensation such as non-linear lens distortions. Prior to the adjustment, the tie points are automatically measured by detecting and matching features in overlapping images resulting in a sparse point cloud (Mayer and Kersten, 2018). The settings in this project were chosen as follows:

- General: Accuracy: Medium; Generic preselection: yes; Reference preselection: yes
- Advanced: Key Point limit: 40000; Tie point limit: 4000; apply mask: no; Adaptive camera model fitting: yes

Sparse cloud filtering was performed under the following settings:

- gradual Selection: reprojection error: 0.26; reconstruction uncertainty: 189.461; projection accuracy: 12.4621; reconstruction uncertainty:6.72951; reprojection error:0.122199

Table 1: **Dates** of the UAV overpasses.

Dates
2019-04-29
2019-05-03
2019-05-10
2019-05-16
2019-06-05
2019-06-20

Based on the information of the point cloud PhotoScan can construct a polygon model (e.g. mesh) (Agisoft, 2019). In this project the mesh was build by the following settings:

- General: surface type: Height field (2.5D); source data: sparse cloud; face count: medium
- Advanced: Interpolation: enabled; Point classes: all; calculate vertex colors

The different pixel values from different photos are combined by the mosaic type in the final texture. Mosaic type implies a two-step approach. Low frequency components are blended for overlapping images to avoid seam line problems. The high-frequency component, on the other hand, which is responsible for the image details, is only captured from a single image.

In total we worked on 6 images which were obtained between the end of April to the end of June (see Table 1). In the mid latitudes of central Europe these are the months of vegetational peak of mixed forests. However, it must be noted, that the images provided by the Nature 4.0 project showed a rather large margin of error when it comes to the accuracy of georefferencing. Therefore, a number of locations in the images are not optimally overlaid, which leads to image distortions. The following figure shows the image distortion for a sample location. This location is not included in our study area, where we suggest the difference of loclizations to be much smaller than in the image below. However, we could not exclude the influence of these distortions completely.

Figure 2: Display of the image distortion in the data basis (The car as well as the rectangle form on the right of the image are visible multiple times at slightly different locations due to the construction of the mesh).

2.3 Tree species data

With the use of a differential GPS the position of tree stems within the study area was logged during a field campaign. Associated with the positional data, the tree species as well as the DBH was collected. As stated before, here we only focused on the determination of the impact of changing resolutions and multi-temporal predictor variables on the classification accuracy. Therefore, we simplified the delineation of tree crowns corresponding to the needs of the investigation. First, we excluded all trees with a DBH below 40 cm, because we assumed that the crowns of greater trees would cover the smaller ones and thus they could not be observed on aerial images from above the crown surface. Secondly, we buffered the central positions of the residual trees by a square of 2 x 2 m, assuming that with this size we would essentially cover substantial proportions of the associated tree crown (**Fig. 1**). However, some of these buffered polygons intersected. In these cases, we decided to exclude both intersecting polygons since any decision to keep one over the other would be arbitrary. In the end, we obtained 161 tree individuals of which 92 (57%) were *fagus sylvatica* and 69 (43%) were *quercus robur*.

2.4 RGB indices

We calculated a number of seven color vegetation indices (VI) which can be found in Table 2. These color indices were suspected to care information content on the phenological development of tree species during a year. Indices are frequently used in remote sensing studies due to their relational nature which compensates for influences of illumination and viewing geometry on the measured reflectance values of the RGB channels. They were calculated for each UAV overpass resulting in (7VIs+R+G+B) x 6 observations = 60 mono-temporal predictor variables. Additionally, we calculated the maximum (MAX), minimum (MIN), sum (SUM), standard deviation (SD), amplitude (AMP) as well as the 25%- (Q25) and 75%-percentile (Q75) values for each VI and the raw channels across the time series resulting in additional 70 seasonal predictors.

Table 2: Names and formulas of RGB indices.

name	abbreviation	formula	reference
Triangular greenness index	TGI	-0.5 * (190*(R-G) - 120*(R-B))	Broge and Leblanc (2001)
Green Leaf Index	GLI	(2*G-R-B) / (2*G+R+B)	Gobron et al. (2000)
Color Index of Vegetation	CIVE	(0.441*R-0.881*G + 0.385*B + 18.787)	Wan et al. (2018)
Iron Oxide Index	IO	R/B	Rowan and Mars (2003)
Visible Vegetation Index	VVI	(1-|R-30| / |R+30|) * (1- |G-50| / |G+50|) * (1-|B-1| / |B+1|)	Planetary Habitability Laboratory (2015)
Green Chromatic Coordinate	GCC	G / (R+G+B)	Sonnentag et al. (2012)
Red Chromatic Coordinate	RCC	R / (R+G+B)	Richardson et al. (2009)

Note:
R: 580-670 nm, G: 480-610 nm, B: 400-520 nm, for digital cameras according to Hunt et al. (2012).

Fig. 3 shows the trajectory of the calculated VIs according to the tree species indicating the mean value (solid line) as well as one standard deviation from the mean (dashed lines) based on all pixels within the respective tree polygons. The trajectories are very similar for both classes, however, for almost all VIs there are substantial differences between the classes during the first observations during the month of May.

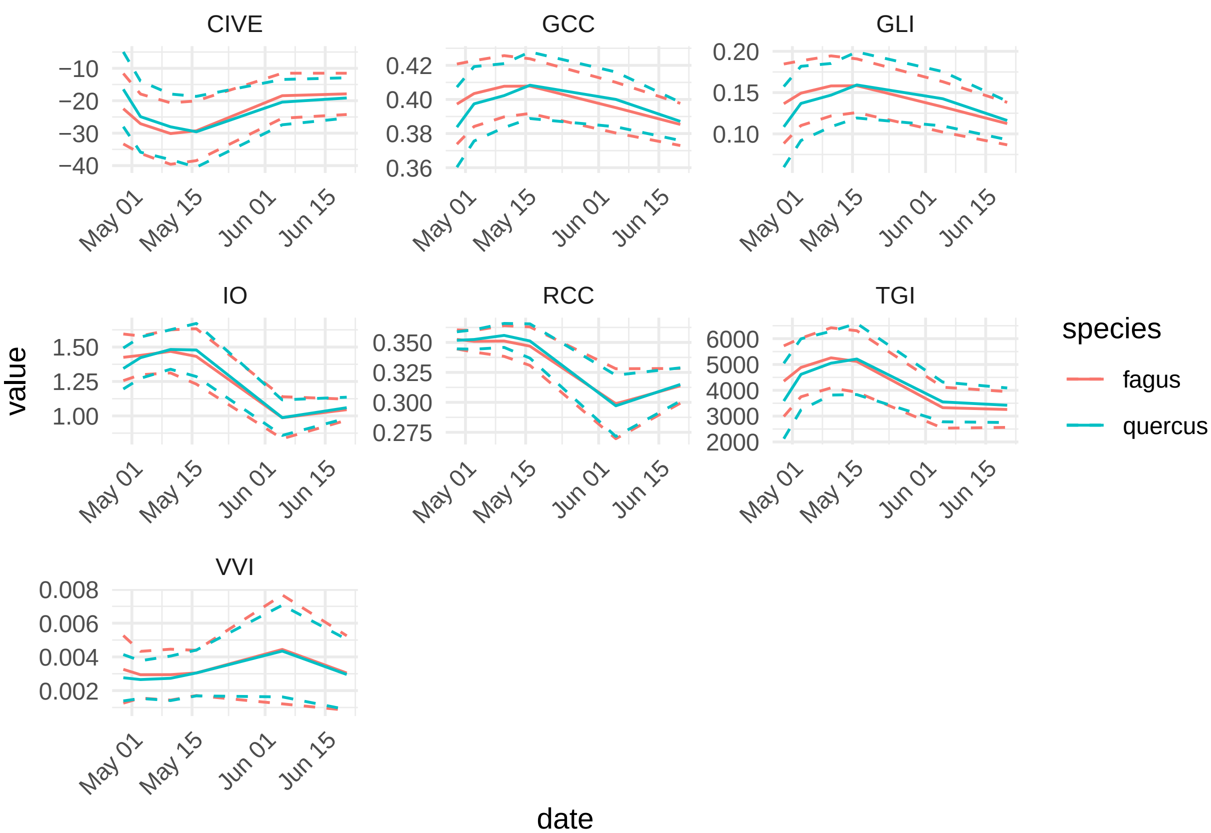

Figure 3: Temporal dynamic of calculated VIs over the course of the year by tree species at 25 cm resolution (dashed lines represent plus and minus one standard deviation).

Concerning the frequency of the seasonal predictor variables both tree species are characterized by a very similar distribution (Fig. 4), however, we see that we have a substantially higher number of pixels classified as *fagus sylvatica* in total.

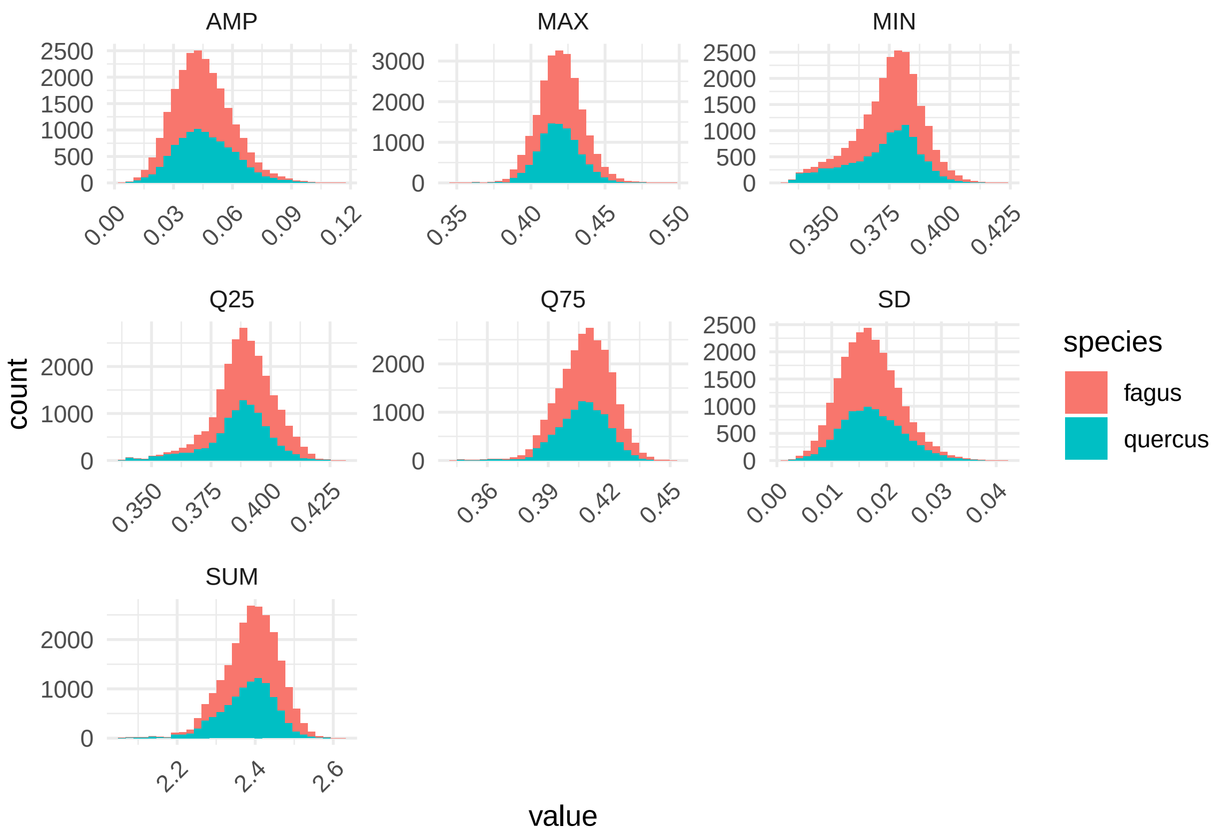

Figure 4: Exampalary histogramm plot of seasonal parameters for RCC by tree species at 25 cm resolution.

2.5 Classification and Validation

For the classification of tree species we used a Random Forest model based on a forward-feature selection of predictor variables stratified by a leave-location-out five-fold cross-validation technique (LLOCV). Random Forest is a non-parametric model, both suitable for regression and classification problems. It was developed by Breiman (2001) and is works by the establishment of a number of decision trees, the forest, each constructed on a random split of predictor variables. The final class decision is made by a majority vote of all trees in the forest. We used the implementation in the `caret` package (Kuhn, 2019) as well as the `CAST` package to implement the LLOCV (Meyer, 2018).

3 Results

To validate the models, the Kappa value is first determined. If the raters agree in all their judgments, the kappa value is equal to 1, and if there are only matches between the two raters that mathematically correspond to the extent of the randomness, it assumes a value of zero (Greve and Wentura, 1997). Kappa values between 0.6 and 0.4 are still considered acceptable, values below 0.40 should be regarded with skepticism. Interrater reliability values of 0.75 are considered good to excellent (Greve and Wentura, 1997).

Figure 5 shows that all models, excluding the model at a 25cm resolution including all variables, regardless of the use of seasonal and vegetation indices and resolution, have a kappa value significantly below the acceptable limit of 0.4. The Kappa value for mono-temporal and seasonal indices increases with decreasing resolution. The comparison shows that the models calculated exclusively with mono-temporal indices show a significantly higher Kappa value than the models calculated exclusively with seasonal indices. Overall, it can be seen that the models with th lowest resolution of 25cm achieve significantly better Kappa values than the models with higher resolutions.

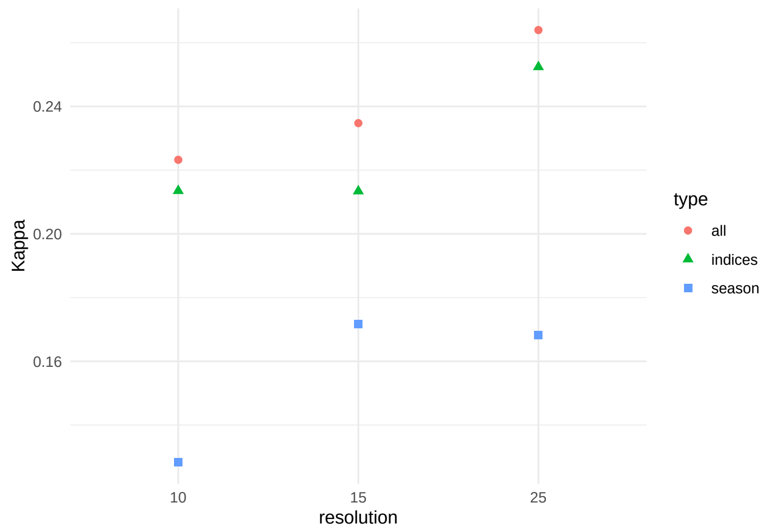

Figure 5: Kappa scores of the random forest models based varying pixel sizes and predictor variables (green - mono-temporal indices, blue - seasonal indices, red - mono-temporal and seasonal indices)

As a another statistical measure of quality, the accuracy of species classification on an object basis is investigated. An object is considered correctly classified if a majority of the pixels belonging to the object corresponds to the class of this object. Figure 6 shows the percentage of objects classified as the correct species based on the majority of pixels within its boundaries. It is clearly shown that, regardless of the variables used, the accuracy of object classification increases from a resolution of 10 cm to a r esolution of 15 cm. The resolution of 20cm, on contrast, has either a negative effect or not effect at all on the accuracy for all models. It is striking that the models where mono-temporal and seasonal indices were used in combination had the lowest accuracy in object classification but achieved the highest Kappa values on a pixels basis (Figure 5).

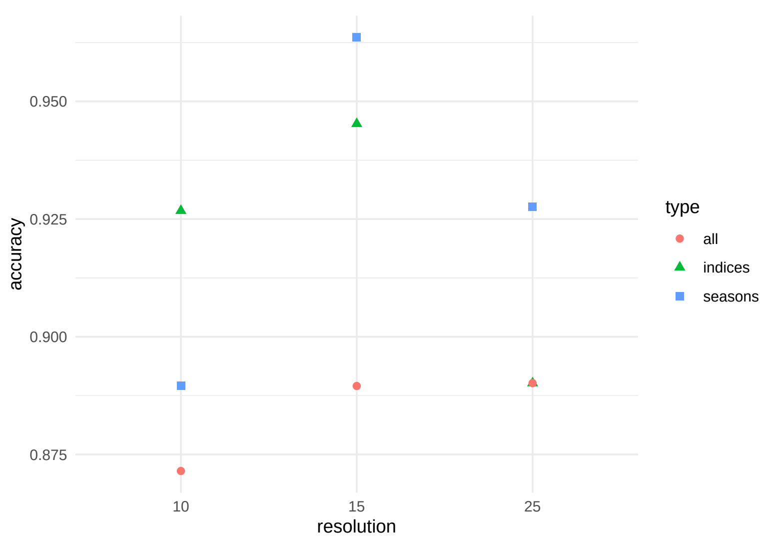

Figure 6: Overall Accuracy of species classification on an object basis.

To generate further insights into the importance of single variables and indices, we evaluated the variable importance. The variable importance describes the explanatory portion a variable has in a given model in percent. Figures 7, 8 and 9 show the predictors and their explanatory portions for the models with mono-temporal indices, seasonal indices and both variable types in combination. The explanation percentages of the individual predictors were calculated from the respective models. The variable with the highest explanatory share is shown as 100%. The explanation share of the remaining variables is shown in relation to this variable with the highest explanation power.

For models with mono-temporal predictors, the GCC, GLI and VVI indices are of particular high importance (Fig. 7). It is noticeable that the aerial photographs of June 5th play an important role in the model calculation. When seasonal predictors are used for model calculation, Figure 8 shows that the RCC index is of great importance. Also, seasonal parameters of the TGI appear three times.

Looking at the explanatory share for models calculated using a combination of mono-temporal and seasonal indices, it is noticeable that significantly more mono-temporal predictors are important than seasonal predictors. Furthermore, it can be seen that the importanve of mono-temporal predictors for model explanation changes in comparison to Figure 7. However, it is observed that the GCC index of April 29th is of higher importance compared to the mono-temporal predictors models only. In addition, completely different predictors, irrespective of whether they are mono-temporal or seasonal, have an influence on the model explanation than in the models with exclusively mono-temporal or seasonal predictors. The importance of predictors for June 5th, however, remains also in the combination models. The situation is similar for the GCC, RCC and VVI indices, which are more frequently present as high importance explanatory variables than other indices.

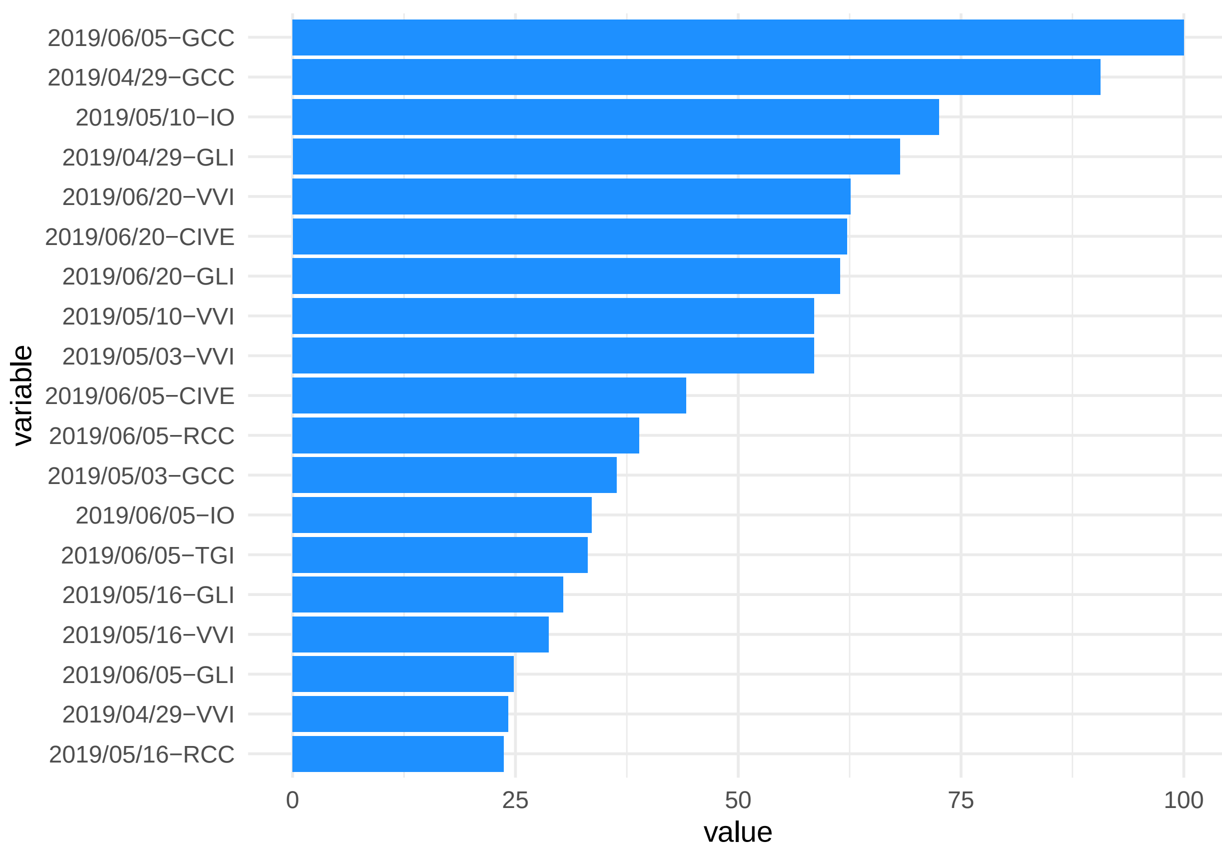

Figure 7: Variable importance for mono-temporal predictors averaged accross resolutions.

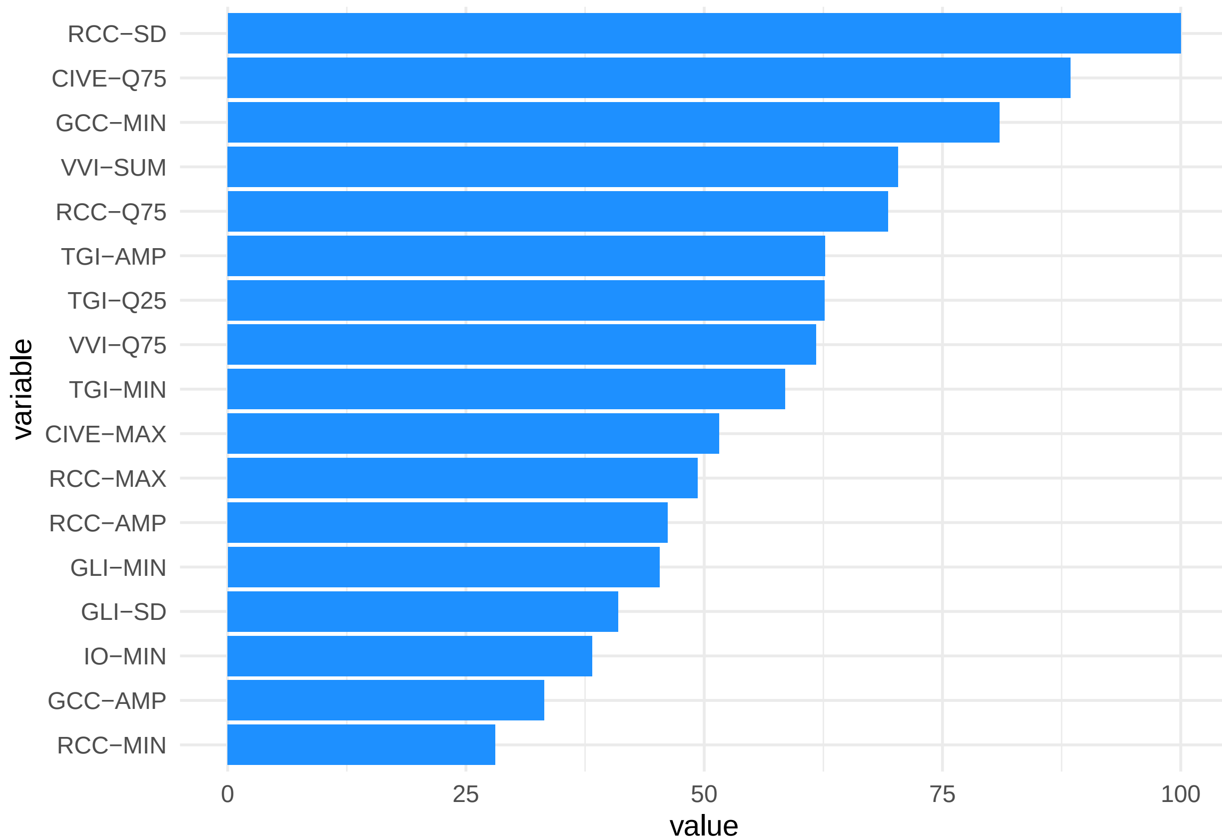

Figure 8: Variable importance for seasonal predictors averaged accross resolutions.

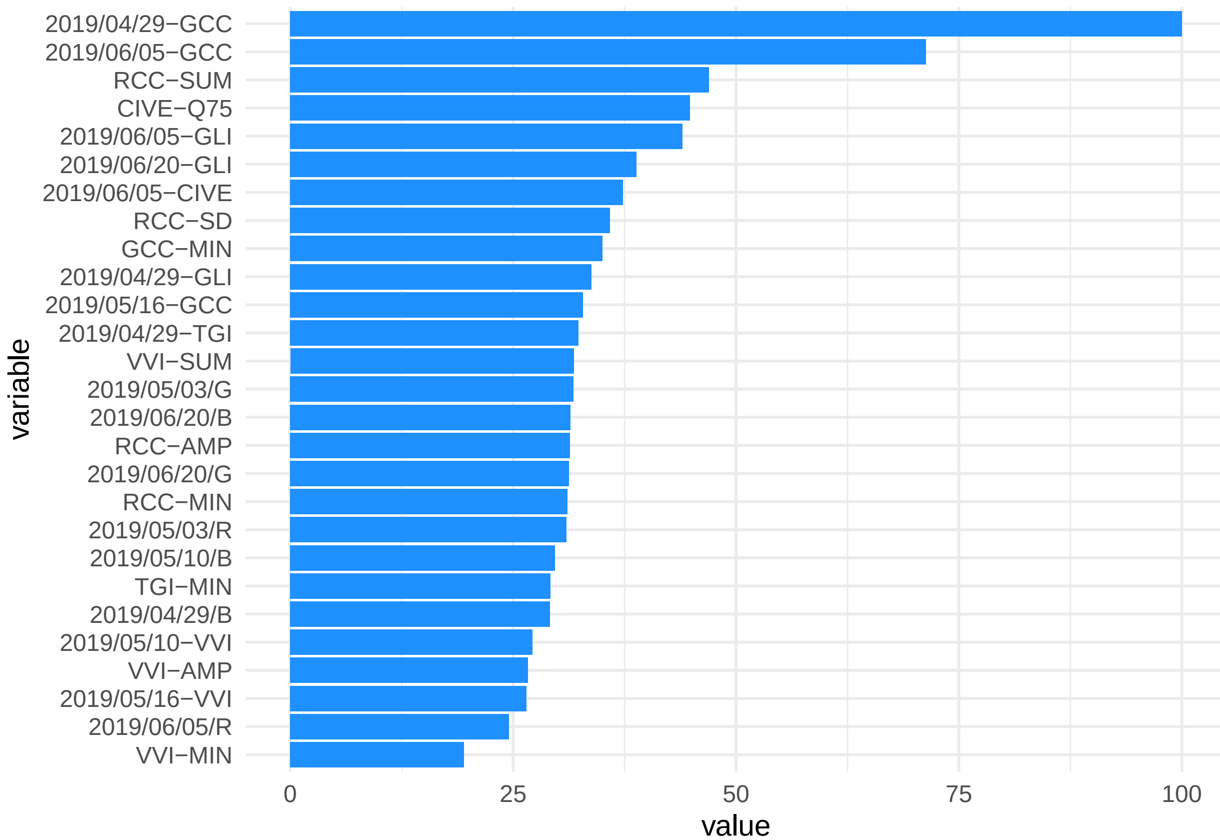

Figure 9: Variable importance for mono-temporal and seasonal predictors averaged accross resolutions.

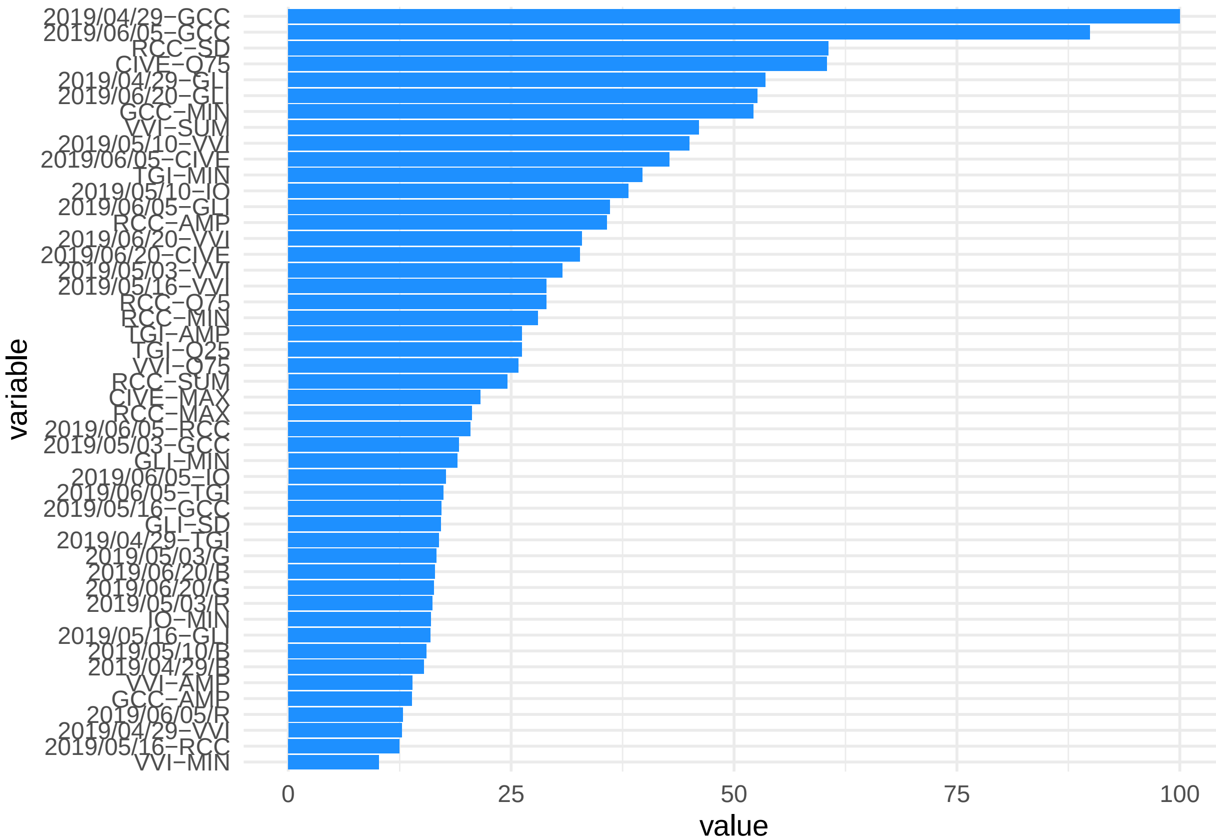

Figure 10: Variable importance across all model types and resoultions.

4 Discussion

The presented results are prone to a number of sources of errors. First, there is the inconsistent georefferencing which led to rather large image distortions (Fig. 2). This error is amplified by a second source of errors, namely the rather coarse localizations of tree crowns within the images (Fig. 1). With the chosen approach in this study, it is possible that pixels which belong to another tree with another species are considered as the wrong class.

The results of the Kappa scores per pixels indicate the potential of the models to classify tree species a little better than by random chance at our study site. The very high accuracies achieved on the object basis, however, indicate that the predictors are capable of modelling tree species. The very high differences between per pixel and object based classification results can be explained through the inclusion of wrongly classifed pixels in the trainig process. This reduces the accuracy of per pixel classification, however, the error can be accounted for by classifiying objects.

Another source of error, closley associated with the very high accuracy results of the object based classification, is the dominance of *fagus sylvatica* in the training dataset. Model performance might solely increase due to a more frequent classification of fagus, since the majority of objects belongs to this class. Another contributing factor amplifing that over representation may be the decreasing spatial resolution, as more pixels belonging to the class *fagus sylvatica* are crunched into bigger sized pixels and thus smoothing out the already underrepresented *quercus robur* pixels.

The present approach thus is in high need for improvment for the localization of training trees. The results of the influences of different resolutions and the incorporation of mono- and seasonal-predictors, still have the potential to highlight valid insights. Models trained with both mono-temporal and seasonal indices performed best overall closely followed by models trained with mono-temporal indices only. Thus leading us to the conclusion, that mono-temporal predictors are more important than seasonal predictors but a combination of both improves model performance slightly. A reason for the rather poor performance of the seasonal parameters might be the temporal resolution of available UAV overpasses. It is possible that with low-frequency observation flights, the important development processes of vegetation growth might not captured and therefore cannot be accounted for in modeling the tree species.

In order to conduct further analysis into that important topic and to bring UAV imagery to good use in tree species classification it is strongly recommended to improve the image pre-processing steps involved in this study in order to minimize the localization error of pixels. Secondly, a robust scheme of crown delination seems to be of high importance in order to get a valid, error-free trainig dataset. Under these conditions, we suspect the gap between the accuracies of pixel-based and object-based classification methods to be smaller.

References

Agisoft, 2019. Agisoft Metashape User Manual 139.

Berra, E.F., Gaulton, R., Barr, S., 2019. Assessing spring phenology of a temperate woodland: A multiscale comparison of ground, unmanned aerial vehicle and Landsat satellite observations. Remote Sensing of Environment 223, 229–242. https://doi.org/10.1016/j.rse.2019.01.010

Berra, E.F., Gaulton, R., Barr, S., 2016. Use of a digital camera onboard a UAV to monitor spring phenology at individual tree level, in: 2016 Ieee International Geoscience and Remote Sensing Symposium (Igarss). pp. 3496–3499. https://doi.org/10.1109/IGARSS.2016.7729904

Breiman, L., 2001. Random forests. Machine learning 45, 5–32. https://doi.org/10.1023/A:1010933404324

Brieger, F., Herzschuh, U., Pestryakova, L.A., Bookhagen, B., Zakharov, E.S., Kruse, S., 2019. Advances in the derivation of Northeast Siberian forest metrics using high-resolution UAV-based photogrammetric point clouds. Remote Sensing 11, 1447. https://doi.org/10.3390/rs11121447

Brockerhoff, E.G., Barbaro, L., Castagneyrol, B., Forrester, D.I., Gardiner, B., González-Olabarria, J.R., Lyver, P.O., Meurisse, N., Oxbrough, A., Taki, H., Thompson, I.D., Plas, F. van der, Jactel, H., 2017. Forest biodiversity, ecosystem functioning and the provision of ecosystem services. Biodiversity and Conservation 26, 3005–3035. https://doi.org/10.1007/s10531-017-1453-2

Broge, N.H., Leblanc, E., 2001. Comparing prediction power and stability of broadband and hyperspectral vegetation indices for estimation of green leaf area index and canopy chlorophyll density. Remote Sensing of Environment 76, 156–172. https://doi.org/10.1016/S0034-4257(00)00197-8

Dostálová, A., Wagner, W., Milenković, M., Hollaus, M., 2018. Annual seasonality in Sentinel-1 signal for forest mapping and forest type classification. International Journal of Remote Sensing 39, 7738–7760. https://doi.org/10.1080/01431161.2018.1479788

Elatawneh, A., Rappl, A., Rehush, N., Schneider, T., Knoke, T., 2013. Forest tree species communities identification using multi phenological stages RapidEye data : case study in the forest of Freising. 5. RESA Workshop 4/2013 1–10.

Food and Agriculture Organsiation of the United Nations, 2015. Global Forest Resources Assessment 2015. https://doi.org/10.1002/2014GB005021

Fricker, G.A., Ventura, J.D., Wolf, J.A., North, M.P., Davis, F.W., Franklin, J., 2019. A Convolutional Neural Network Classifier Identifies Tree Species in Mixed-Conifer Forest from Hyperspectral Imagery. Remote Sensing 11, 2326. https://doi.org/10.3390/rs11192326

Frison, P.L., Fruneau, B., Kmiha, S., Soudani, K., Dufrêne, E., Le Toan, T., Koleck, T., Villard, L., Mougin, E., Rudant, J.P., 2018. Potential of Sentinel-1 data for monitoring temperate mixed forest phenology. https://doi.org/10.3390/rs10122049

Gobron, N., Pinty, B., Verstraete, M.M., Widlowski, J.L., 2000. Advanced vegetation indices optimized for up-coming sensors: design, performance, and applications. IEEE Transactions on Geoscience and Remote Sensing 38, 2489–2505. https://doi.org/10.1109/36.885197

Grabska, E., Hostert, P., Pflugmacher, D., Ostapowicz, K., 2019. Forest stand species mapping using the sentinel-2 time series. Remote Sensing 11, 1–24. https://doi.org/10.3390/rs11101197

Greve, W., Wentura, D., 1997. Wissenschaftliche Beobachtung.

Hunt, E.R., Doraiswamy, P.C., McMurtrey, J.E., Daughtry, C.S., Perry, E.M., Akhmedov, B., 2012. A visible band index for remote sensing leaf chlorophyll content at the Canopy scale. International Journal of Applied Earth Observation and Geoinformation 21, 103–112. https://doi.org/10.1016/j.jag.2012.07.020

Klosterman, S., Richardson, A.D., 2017. Observing spring and fall phenology in a deciduous forest with aerial drone imagery. Sensors (Switzerland) 17. https://doi.org/10.3390/s17122852

Krause, S., Sanders, T.G., Mund, J.P., Greve, K., 2019. UAV-based photogrammetric tree height measurement for intensive forest monitoring. Remote Sensing 11, 758. https://doi.org/10.3390/rs11070758

Kuhn, M., 2019. Caret: Classification and regression training, https://CRAN.R-project.org/package=caret.

Laboratory, P.H., 2015. Visible Vegetation Index (VVI).

Marques, P., Pádua, L., Adão, T., Hruška, J., Peres, E., Sousa, A., Sousa, J.J., 2019. UAV-based automatic detection and monitoring of chestnut trees. Remote Sensing 11, 855. https://doi.org/10.3390/RS11070855

Mayer, C., Kersten, T.P., 2018. A Comprehensive Workflow to Process UAV Images for the Efficient Production of Accurate Geo-information A Comprehensive Workflow to Process UAV Images for the Efficient Production of Accurate Geo-information.

Meyer, H., 2018. CAST: 'Caret' applications for spatial-temporal models, https://CRAN.R-project.org/package=CAST.

Mngadi, M., Odindi, J., Peerbhay, K., Mutanga, O., 2019. Examining the effectiveness of Sentinel-1 and 2 imagery for commercial forest species mapping. Geocarto International 0, 1–12. https://doi.org/10.1080/10106049.2019.1585483

Natesan, S., Armenakis, C., Vepakomma, U., 2019. Resnet-based tree species classification using uav images. International Archives of the Photogrammetry, Remote Sensing and Spatial Information Sciences - ISPRS Archives 42, 475–481. https://doi.org/10.5194/isprs-archives-XLII-2-W13-475-2019

Nevalainen, O., Honkavaara, E., Tuominen, S., Viljanen, N., Hakala, T., Yu, X., Hyyppä, J., Saari, H., Pölönen, I., Imai, N.N., Tommaselli, A.M., 2017. Individual tree detection and classification with UAV-Based photogrammetric point clouds and hyperspectral imaging. Remote Sensing 9. https://doi.org/10.3390/rs9030185

Niculescu, S., Talab Ou Ali, H., Billey, A., 2018. Random forest classification using Sentinel-1 and Sentinel-2 series for vegetation monitoring in the Pays de Brest (France), in:. p. 6. https://doi.org/10.1117/12.2325546

Persson, M., Lindberg, E., Reese, H., 2018. Tree species classification with multi-temporal Sentinel-2 data. Remote Sensing 10, 1–17. https://doi.org/10.3390/rs10111794

Richardson, A.D., Braswell, B.H., Hollinger, D.Y., Jenkins, J.P., Ollinger, S.V., 2009. Near-surface remote sensing of spatial and temporal variation in canopy phenology. Ecological Applications 19, 1417–1428. https://doi.org/10.1890/08-2022.1

Rowan, L.C., Mars, J.C., 2003. Lithologic mapping in the Mountain Pass, California area using Advanced Spaceborne Thermal Emission and Reflection Radiometer (ASTER) data. Remote Sensing of Environment 84, 350–366. https://doi.org/10.1016/S0034-4257(02)00127-X

Sonnentag, O., Hufkens, K., Teshera-Sterne, C., Young, A.M., Friedl, M., Braswell, B.H., Milliman, T., O'Keefe, J., Richardson, A.D., 2012. Digital repeat photography for phenological research in forest ecosystems. Agricultural and Forest Meteorology 152, 159–177. https://doi.org/10.1016/j.agrformet.2011.09.009

Sothe, C., Dalponte, M., Almeida, C.M. de, Schimalski, M.B., Lima, C.L., Liesenberg, V., Miyoshi, G.T., Tommaselli, A.M.G., 2019. Tree species classification in a highly diverse subtropical forest integrating UAV-based photogrammetric point cloud and hyperspectral data. Remote Sensing 11, 1338. https://doi.org/10.3390/rs11111338

Ulsig, L., Nichol, C.J., Huemmrich, K.F., Landis, D.R., Middleton, E.M., Lyapustin, A.I., Mammarella, I., Levula, J., Porcar-Castell, A., 2017. Detecting inter-annual variations in the phenology of evergreen conifers using long-term MODIS vegetation index time series. Remote Sensing 9. https://doi.org/10.3390/rs9010049

Wan, L., Li, Y., Cen, H., Zhu, J., Yin, W., Wu, W., Zhu, H., Sun, D., Zhou, W., He, Y., 2018. Combining UAV-based vegetation indices and image classification to estimate flower number in oilseed rape. Remote Sensing 10. https://doi.org/10.3390/rs10091484

Yan, W., Guan, H., Cao, L., Yu, Y., Gao, S., Lu, J.Y., 2018. An automated hierarchical approach for three-dimensional segmentation of single trees using UAV LiDAR data. Remote Sensing 10, 1999. https://doi.org/10.3390/rs10121999

Yao, H., Qin, R., Chen, X., 2019. Unmanned aerial vehicle for remote sensing applications - A review. https://doi.org/10.3390/rs11121443

Zhang, X., Friedl, M.A., Schaaf, C.B., Strahler, A.H., Hodges, J.C., Gao, F., Reed, B.C., Huete, A., 2003. Monitoring vegetation phenology using MODIS. Remote Sensing of Environment 84, 471–475. https://doi.org/10.1016/S0034-4257(02)00135-9